

OPEN

Prokineticin receptor 2 affects GnRH3 neuron ontogeny but not fertility in zebrafish

Ivan Bassi¹, Francesca Luzzani¹, Federica Marelli^{1,2}, Valeria Vezzoli¹, Ludovica Cotellessa^{1,2}, David A. Prober³, Luca Persani^{1,2}, Yoav Gothilf⁴ & Marco Bonomi² ✉

Prokineticin receptors (PROKR1 and PROKR2) are G protein-coupled receptors which control human central and peripheral reproductive processes. Importantly, allelic variants of *PROKR2* in humans are associated with altered migration of GnRH neurons, resulting in congenital hypogonadotropic hypogonadism (CHH), a heterogeneous disease characterized by delayed/absent puberty and/or infertility. Although this association is established in humans, murine models failed to fully recapitulate the reproductive and olfactory phenotypes observed in patients harboring *PROKR2* mutations. Here, taking advantage of zebrafish model we investigated the role of *prokr1b* (ortholog of human *PROKR2*) during early stages of GnRH neuronal migration. Real-Time PCR and whole mount *in situ* hybridization assays indicate that *prokr1b* spatial-temporal expression is consistent with *gnrh3*. Moreover, knockdown and knockout of *prokr1b* altered the correct development of GnRH3 fibers, a phenotype that is rescued by injection of *prokr1b* mRNA. These results suggest that *prokr1b* regulates the development of the GnRH3 system in zebrafish. Analysis of gonads development and mating experiments indicate that *prokr1b* is not required for fertility in zebrafish, although its loss determine changes also at the testis level. Altogether, our results support the thesis of a divergent evolution in the control of vertebrate reproduction and provide a useful *in vivo* model for deciphering the mechanisms underlying the effect of *PROKR2* allelic variants on CHH.

The hypothalamus-pituitary-gonadal (HPG) axis controls reproduction in vertebrates^{1–5} through the pulsatile release of gonadotropin-releasing hormone (GnRH) hormone by GnRH neurons. During development, these neurons differentiate from neural crest cells and ectodermal progenitors in a niche at the border between the respiratory epithelium and the vomeronasal/olfactory epithelium. From these regions these neurons migrate caudally to reach the medio-basal hypothalamus, where they complete their differentiation⁶. Several studies in different animal models have shown that specific evolutionarily conserved genes regulate this migratory process and the functions of these neurons. The role of these genes in human fertility is supported by the existence of variants in these genes associated with congenital hypogonadotropic hypogonadism (CHH)⁷, a rare and clinically heterogeneous disorder characterized by abnormal pubertal development and/or infertility, a normal (nCHH) or defective sense of smell (Kallmann syndrome, KS) and other reproductive and non-reproductive anomalies^{8–10}. More than 25 genes have been associated with CHH, although variants in these genes account only for 40–50% of reported cases. Several evidences indicate that CHH is a complex genetic disease characterized by variable expressivity and penetrance of the associated genetic defects, which can be partially explained by an oligogenic-inheritance model^{9,11}. Among the genes involved in CHH, prokineticin receptor 2 (*PROKR2*) has an important role in GnRH neuron migration. *PROKR2*, as a member of the GPCR family, has an extracellular amino-terminal end, an intracellular carboxy-terminal domain and a central core formed by seven transmembrane α -helical segments (TM1–TM7)¹². Prokineticins have been previously demonstrated to be involved in several physiological functions in neurogenesis, regulation of circadian rhythms, metabolism, angiogenesis, pain perception, muscle contractility, hematopoiesis, immune response, thermoregulation and energy expenditure^{13–15}. Matsumoto and colleagues in 2006 reported the first observation that *Prokr2* knock-out mice display hypoplastic gonads and

¹IRCCS Istituto Auxologico Italiano, Division of Endocrine and Metabolic Diseases & Lab. of Endocrine and Metabolic Research, Milan, Italy. ²Department of Clinical Sciences and Community Health, University of Milan, Milan, Italy. ³Division of Biology and Biological Engineering, California Institute of Technology, Pasadena, CA, USA. ⁴Department of Neurobiology, The George S. Wise Faculty of Life Sciences and Sagol School of Neuroscience, Tel-Aviv University, Tel-Aviv, Israel. ✉e-mail: m.bonomi@auxologico.it

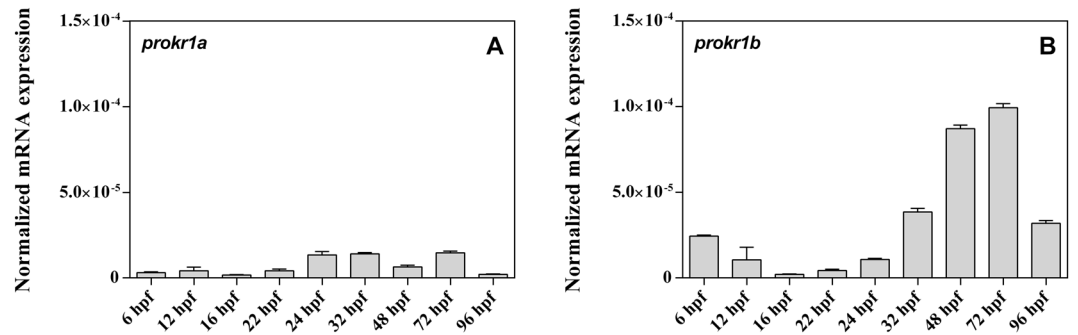


Figure 1. Real-time-PCR experiments show that during GnRH3 neuron development *prokr1a* (A) is less expressed compared to *prokr1b* (B). (gene were normalized using *efl1a* as housekeeping gene. For each developmental stage $n = 20$).

olfactory structures, a phenotype reminiscent of KS, to link this gene to CHH¹⁶. Furthermore, *Prokr2* knock-out mice show decreased plasma levels of testosterone and follicle-stimulating hormone, but not luteinizing hormone. In humans, genetic screening of CHH cohorts has revealed mutations in *PROKR2* in KS and nCHH patients, but mostly in the heterozygous state^{17–20}. Moreover, studies on transfected cells demonstrated that the missense *PROKR2* variants observed in KS and nCHH patients have a deleterious effect on *PROKR2* signaling^{18,20,21} although such variants are also present in apparently unaffected individuals^{22–24}. Thus, despite several *in vitro* and *in vivo* studies, the role of *Prokr2* in GnRH neuron function and in CHH pathogenesis remains incompletely understood. Here, we take advantage of the zebrafish to generate an *in vivo* model to investigate *PROKR2* function during GnRH neuron ontogeny. Using both transient knockdown and germline knockout of *prokr1b*, the zebrafish ortholog of human *PROKR2*, we find that *prokr1b* has an important role in the migration of GnRH axons, but not for fertility, in this animal model.

Results

Mammals possess two prokineticin receptors named *PROKR1* and *PROKR2*²⁵. The zebrafish genome contains two *prokr* paralogs named *prokr1a* and *prokr1b* (or *prokr1l*), and previous evidence suggests that *prokr1a* and *prokr1b* correspond to mammalian *PROKR1* and *PROKR2*, respectively²⁶. To determine which of these genes may be involved in GnRH neuronal migration, we evaluated their expression during zebrafish embryo development. Real-Time PCR analysis on RNA extracts from whole embryos revealed that *prokr1b* is expressed at higher levels compared to *prokr1a* and exhibits an increase from 24 hours post-fertilization (hpf) to 72 hpf (Fig. 1A,B).

Whole-mount *in situ* hybridization (WISH) performed at the same developmental stages (Fig. 2) revealed that *prokr1b*, but not *prokr1a*, is expressed in cells adjacent to the olfactory placodes (Fig. 2G–L), similar to the pattern observed for *gnrh3* (Fig. 2M–R). Given the role of *PROKR2* in the migration of GnRH neurons in humans, these results suggest that *prokr1b* may similarly be involved in GnRH3 neuron development in zebrafish.

Next we used morpholino anti-sense oligonucleotides (MOs) to knock-down expression of *prokr1a* or *prokr1b* in *tg (gnrh3:EGFP)* embryos, which express EGFP in GnRH3 cells²⁷ (Supplementary Fig. S1A–C). Images collected at 48 hpf (Fig. 3) revealed that *prokr1a* knock-down (Fig. 3C) did not affect the development of GnRH3 fibers that appeared similar to those of uninjected wild-type animals (WT, Fig. 3A) or injected with a control MO (*ctrl-MO*) (Fig. 3B). In contrast, knock-down of *prokr1b* led to evident alterations in the architecture of the GnRH3 network (Fig. 3D). In these embryos, GnRH3 fibers appeared disorganized, especially at the level of the anterior commissure (AC) and in the anterior fibers (dotted square in Fig. 3D; Supplementary Fig. S1D). These results suggest that *prokr1b* is required for normal GnRH neuron development in zebrafish.

To confirm the defects observed for *prokr1b* knock-down using MOs, a technique that is prone to non-specific artefacts, we next analyzed GnRH3 neuron development in animals containing a germline mutation in *prokr1b*²⁶. To do so, we compared EGFP-expressing GnRH3 neuron fibers in *prokr1b* homozygous mutant, heterozygous mutant, and homozygous WT siblings at 48 hpf and 72 hpf. No differences were observed between *prokr1b*^{+/-} and WT siblings at these two time points (Fig. 4A,B,E,F), while *prokr1b*^{-/-} embryos (Fig. 4C,G) showed defects in GnRH3 neuron fibers in the same anatomical region as in the knockdown experiments (Fig. 3D). This phenotype appears to be specific to the absence of *prokr1b*, as injection of WT *prokr1b*, but not *prokr1a* mRNA into *prokr1b*^{-/-} animals at the 1-cell stage rescued the phenotype (Fig. 4D–H; Supplementary Fig. S2E,F).

These observations were supported by quantitative analysis of GnRH3 neuron fibers (Fig. 5A,B), providing an evidence for a role of *prokr1b* in GnRH neuron development in zebrafish.

In order to establish whether *prokr1b* is required for the development and function of the reproductive system in zebrafish, as it is in humans and mice, we compared the reproductive organs and fecundity of *prokr1b*^{-/-}, *prokr1b*^{+/-} and *prokr1b*^{+/+} siblings. Histological sections of testes and ovaries of 3-months-old male and female animals did not reveal obvious differences among the three genotypes, suggesting that *prokr1b* is not required for gonadal maturation in both sexes and, by consequence, for puberty in zebrafish (Fig. 6A–L). No differences were also observed among the three genotypes in the number of fertile eggs generated (Fig. 6M), neither in the GSI index of mutated male or female compared to WT indicating that *prokr1b* is not fundamental for fertility in zebrafish (Fig. 6N). Nevertheless, Real-Time qPCR conducted on tissue of adult fish, revealed for mutated males

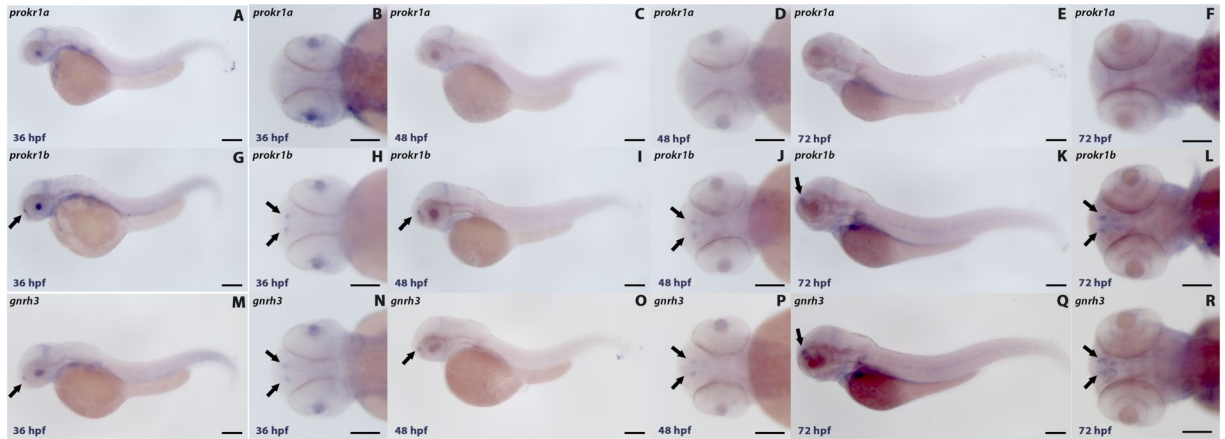


Figure 2. Whole-mount *in situ* hybridization with *prokr1a* probe (A–F) did not display any signal in the head of zebrafish embryos. In contrast, *prokr1b* (G–L) is expressed in cells near the olfactory region at 36 hpf (G,H), 48 hpf (I,J) and 72 hpf (K,L). That is similar to *gnrh3* expression at these times (M–R). Panels A,C,E,G,I,K,M,O and Q show lateral views. Panels B,D,F,H,J,L,N,P and R show dorsal views of zebrafish embryos. Scale bar = 50 μ m. Image taken using Leica Application Suite software (LAS version 4.7.0; <https://www.leica-microsystems.com/products/microscope-software/p/leica-application-suite/>).

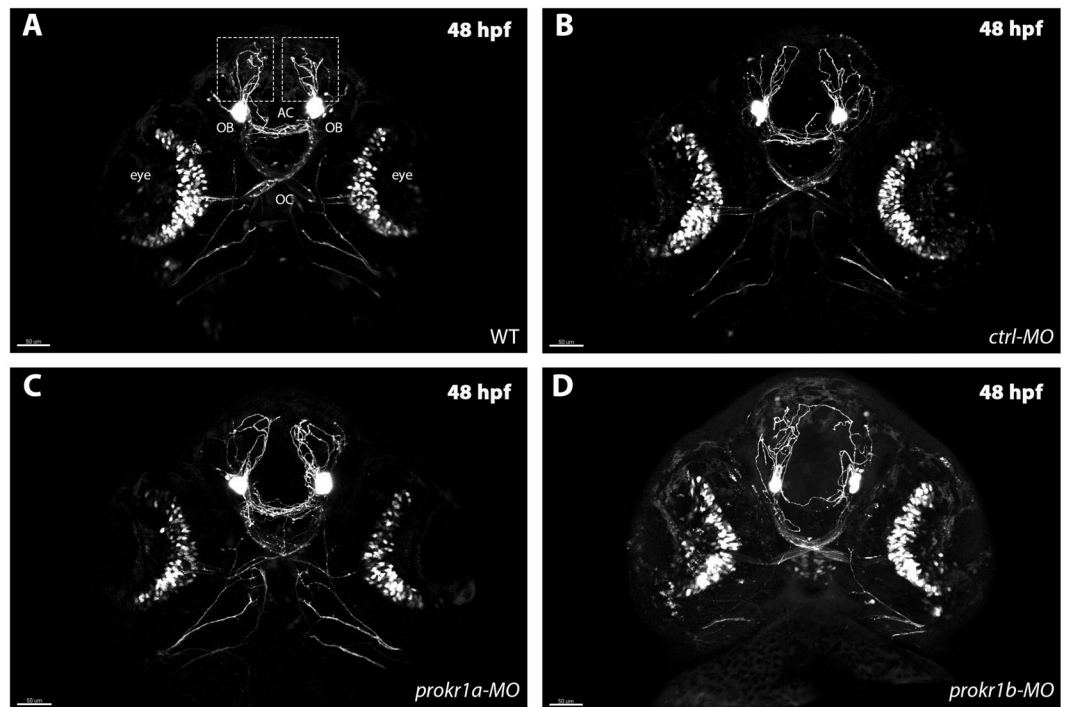


Figure 3. Injection of *ctrl-MO* (B) or *prokr1a-MO* (C) does not affect GnRH3 neuron fibers, as they look comparable to uninjected WT (A) embryos. In contrast, knockdown of *prokr1b* (D) causes alteration in axons migration of the rostral part (dotted square in Fig A) and at the level of the anterior commissure (AC) of the embryos. OB = olfactory bulbs, OC = optic chiasm, AC = anterior commissure. Scale bar = 50 μ m.

higher expression of *lh β* and *fsh β* in the brain (Fig. 6O) together with a strong decrease of the gonadotropic receptors *lhr* and *fshr* in the gonads (Fig. 6P).

Discussion

Several recent studies have demonstrated a remarkable evolutionary conservation of the developmental migration of GnRH neurons and of several genes involved in GnRH ontogeny^{28–31}. In zebrafish, like in mammals, GnRH secreting neurons starts their development at 24 hpf from cells located in the olfactory epithelium that send dorsal extensions that ultimately innervate the hypothalamus and pituitary. An important gene involved

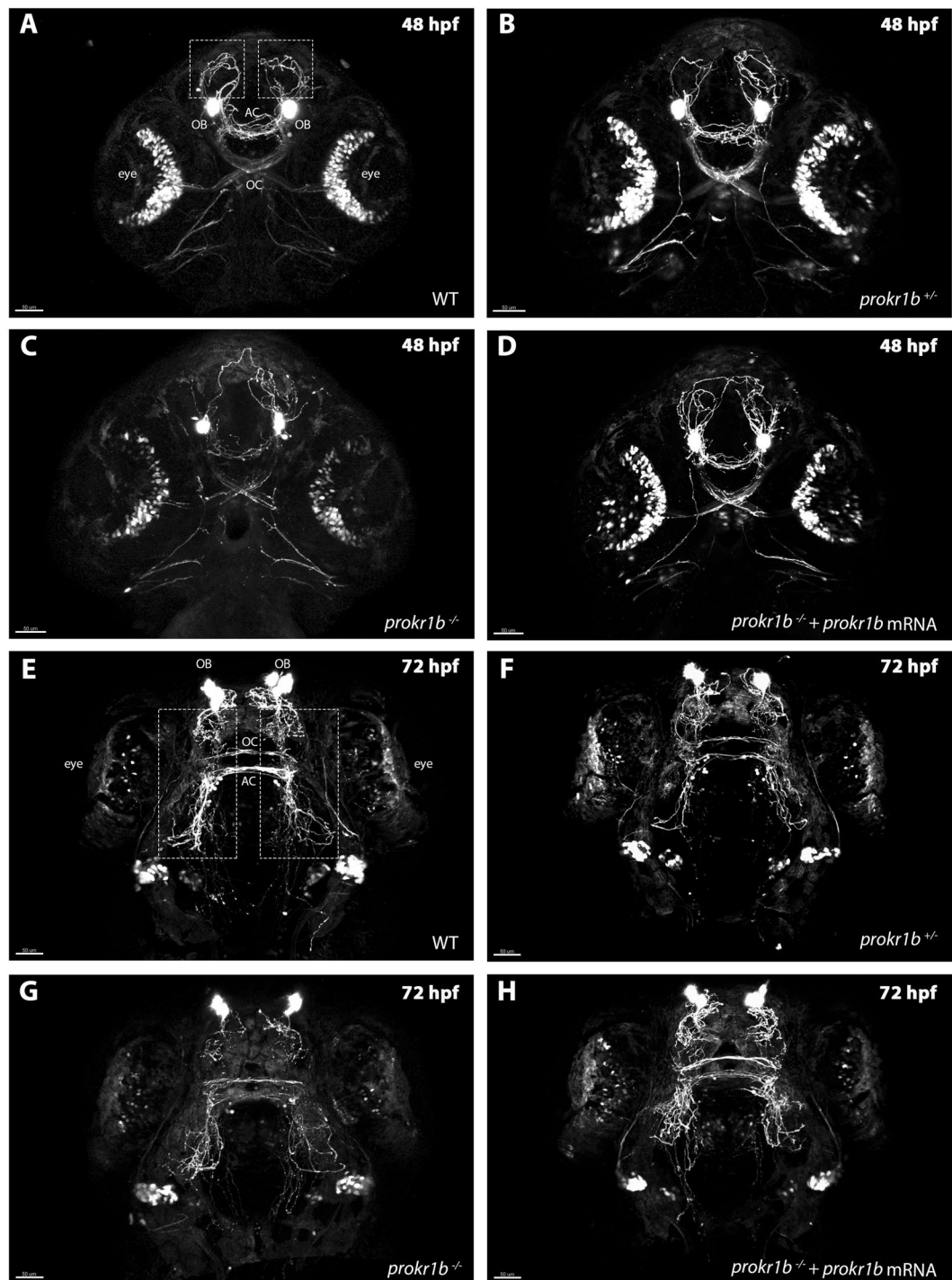


Figure 4. *prokr1b* homozygous mutant zebrafish (*tg(gnrh3:EGFP);prokr1b^{-/-}* (C,G) exhibit misrouting of rostral (dotted square) and optic chiasm (OC) fibers. These defects are not present in WT (A,E) and *prokr1b* heterozygous mutants (*tg(gnrh3:EGFP);prokr1b^{+/-}* (B,F). The *prokr1b* mutant phenotype is rescued by injection with WT *prokr1b* mRNA (D,H). OB = olfactory bulbs, OC = optic chiasm, AC = anterior commissure. Scale bar = 50 μ m.

in the development of the GnRH system in humans is *PROKR2*. The zebrafish genome contains two *prokineticin receptor* paralogues, *prokr1a* and *prokr1b*²⁶. WISH analyses reveal that *prokr1b* expression starts in the brain at 24 hpf close to the olfactory bulbs and appears similar to that of *gnrh3* at 48 and 72 hpf. Accordingly, Real-Time PCR data show that during this time window *prokr1b* expression increases and then drastically decreases at 96 hpf. At 72 hpf, the development of GnRH3 fibers is complete and is followed by the migration of GnRH3 somata from the olfactory region to the hypothalamus²⁷. Consistent with the possibility that zebrafish *prokr1b* is an ortholog of human *PROKR2*, knockdown of *prokr1b*, but not *prokr1a*, affected the formation of rostral GnRH3

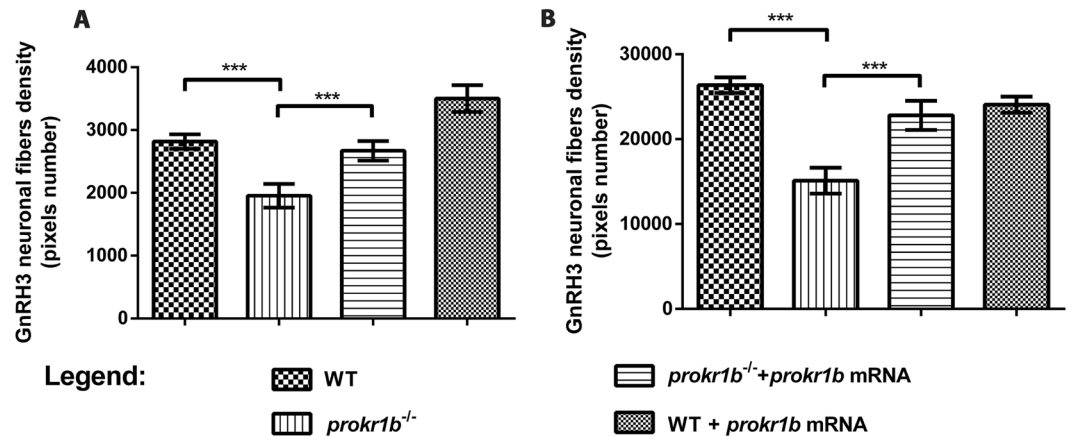


Figure 5. Quantification of GnRH3 fiber network confirms that *prokr1b*^{-/-} embryos have reduced GnRH3 neuron projections, and that this phenotype is rescued by injection of *prokr1b* mRNA when analyzed at 48 hpf (A) or 72 hpf (B). For each group n = 10 animals. ns: not significant, ***p < 0.01.

fibers, similar to humans with *PROKR2* mutations. Importantly, similar defects were also present in homozygous *prokr1b* mutant embryos at 48 hpf, and this phenotype was rescued by injection of WT *prokr1b* mRNA. Taken together, these results demonstrate that *prokr1b* is important for the correct migration of GnRH3 neuron fibers.

Although *prokr1b* appears to be the zebrafish ortholog of human and murine *PROKR2*, the zebrafish *prokr1b* mutant phenotype does not fully recapitulate the clinical features of CHH. Indeed, *prokr1b* mutation does not affect gonadal maturation or fertility in zebrafish, as demonstrated by fecundity testing and histological analysis of testis and ovaries at 3 months of age. Moreover, dorsoventral projections of GnRH3 neurons, despite reduced, are present in zebrafish *prokr1b* mutants at 72 hpf, in contrast to murine *Prokr2* mutants in which there is an early arrest in GnRH neuronal migration¹⁶. Two recent studies conducted in zebrafish have highlighted differences in the role of the GnRH system during puberty and fertility. Liu and colleagues showed that triple mutants lacking *gnrh3* and the 2 kisspeptin ligands undergo normal puberty and gonad maturation³². These results are surprising, because GnRH3 has been considered the most important stimulator of gonadotropin release in fish and its expression, together with *kiss1* and *kiss2*, have been found to be higher during puberty and gonadal maturation in zebrafish³³. Moreover Marvel and colleagues demonstrated that zebrafish *gnrh2/gnrh3* double mutants show normal fertility, demonstrating that neither GnRH2, nor Kiss1 and Kiss2, compensate for loss of GnRH3 in zebrafish³⁴. Nevertheless, comparison between WT and double or triple mutants revealed in both studies different expression patterns of neuropeptides known to be important in mammal control of reproduction, such as *tachykinin 3*, *secretogranin II* and *neuropeptide Y*. These results suggest that, in contrast with mammals, multiple factors act in parallel with GnRH to stimulate the reproductive axis in zebrafish^{32,34,35}. Our results in the knockout male fish might further confirm this hypothesis. Indeed, we reported a *lhr* and *fshr* lower expression in the testis that could firstly indicate a role of *prokr1b* in this organ similar to what already observed in mice, where absence of *Prokr2* lead to a variable degree of compromised vasculature, even in the absence of evident structural gonadal modification³⁶. Moreover, this could also be related to primary testes defect that has been described, in association to those in the hypothalamus and pituitary, also in human male with CHH (Sykiotis *et al.* JCEM 2010). Secondly, this reduced receptor expression might lead to a relative resistance to Lh and Fsh action which, in turn, might activate, through the negative feedback mechanism, the central compartment of the HPG axis. Higher *lhβ* and *fshβ* expression levels in our male knockout fish, seem to confirm this stimulation, nevertheless they are not consequence of level modification in *gnrh3* expression levels. Thus, other factors from GnRH3 system might be implicated in the stimulation of the pituitary as previously suggested^{32,34,35}.

In conclusion, even if mechanisms controlling the HPG and, by consequence, fertility have slightly diverged along evolution, these studies together demonstrate that genes regulating GnRH ontogeny present a certain degree of conservation among humans, mice and zebrafish^{37,38}. Indeed, despite the variable phenotypic features, the *Tg(gnrh3:EGFP);prokr1b^{ct814/ct814}* line presented here suggests that *prokr1b* is the orthologue of human *PROKR2*, and demonstrates that its loss affects the development of GnRH neuronal fibers in zebrafish, as in humans, but also the expression of the *lhr* and *fshr* at the testes level, thus indicating a complex implication of the prokineticin pathway in the HPG functionality. Moreover, this mutant line is a useful *in vivo* tool that, combined with mutant lines for other GnRH related genes, could contribute to our understanding of the development of the GnRH system and the complex mechanisms underlying CHH and related diseases.

Methods

Zebrafish lines and maintenance. Zebrafish (*Danio rerio*) embryos obtained from natural spawning were raised and maintained according to established techniques³⁹. All experiments with live animals were performed at the University of Milan. All experimental protocols and methods were carried out in accordance with relevant guidelines and regulations of Good Animal Practice approved by the institutional and licensing committee IACUC (Institutional Animal Care and Use Committee) and University of Milan by the Italian Decree of March 4th, 2014, n.26. Embryos were staged according to morphological criteria⁴⁰. Beginning from 24 hpf, embryos

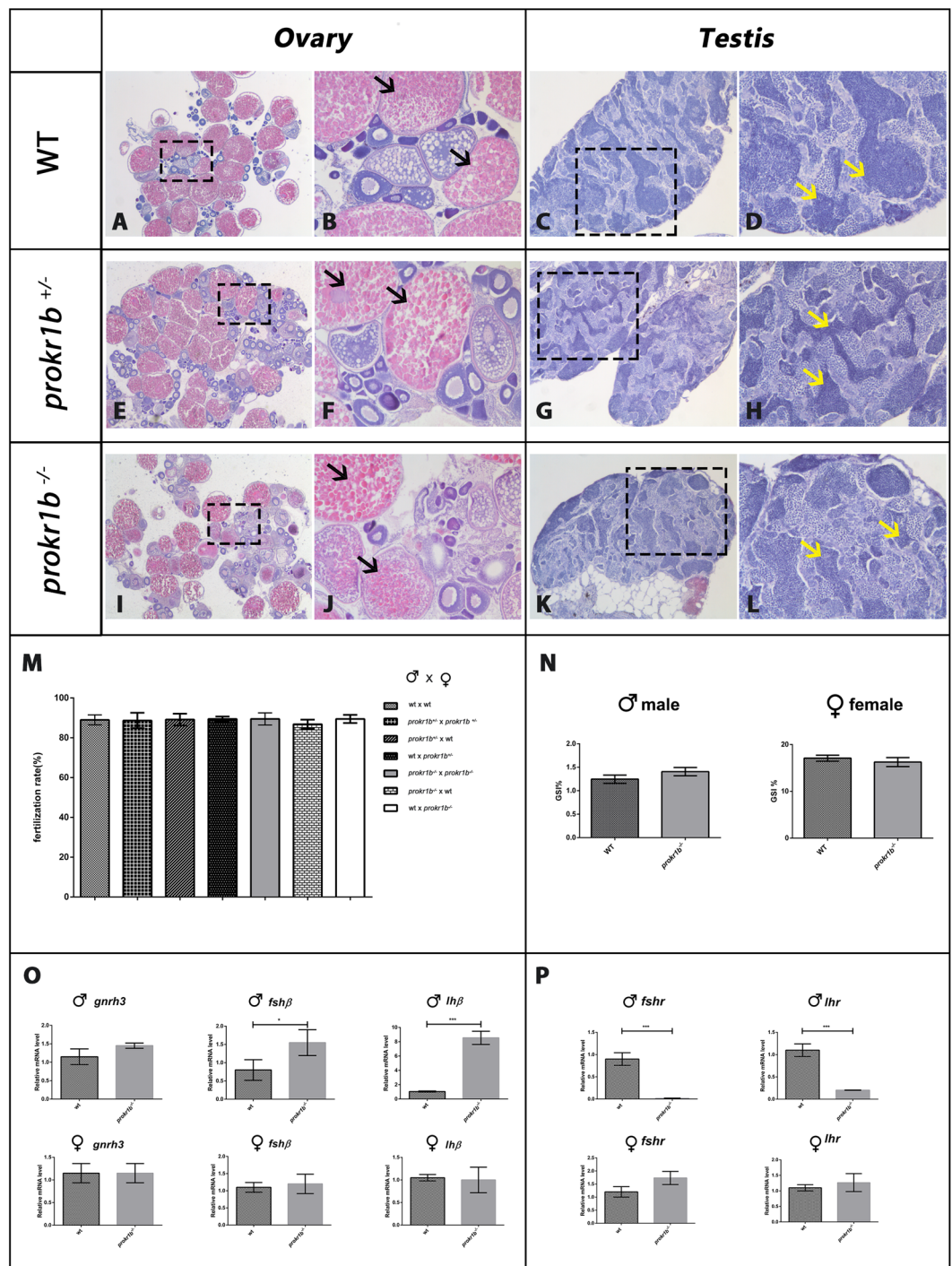


Figure 6. Histological sections conducted on 3 months of age fish showed no defects in the structure of gonads and testis between WT (A,C), heterozygous (E,G) and homozygous mutant (I,K). Sections zoom revealed fully mature oocytes (black arrows in B,F,J) and fully mature spermatozoa (yellow arrows in D,H,L) in WT, *prokr1b*^{+/-} and *prokr1b*^{-/-} animals. Comparison of reproductive outputs (M) and GSI index (N) revealed no differences between WT, heterozygous and homozygous mutants. Real-Time PCR conducted on brain (O) and gonads (P) of WT and mutant fish showed a different expression of *lhβ*, *fshβ*, *lhr* and *fshr* in *prokr1b*^{-/-} males. Image taken using Leica Application Suite software (LAS version 4.7.0; URL: <https://www.leica-microsystems.com/products/microscope-software/p/leica-application-suite/>).

were cultured in fish water containing 0.003% PTU (1-phenyl-2-thiourea; Sigma-Aldrich, Saint Louis, MO) to prevent pigmentation and 0.01% methylene blue to prevent fungal growth³⁹. Wild-type (WT) zebrafish of the AB strain were obtained from the Wilson lab (University College London, London, United Kingdom). The *tg* (*gnrh3:EGFP*)²⁷ and *prokr1b*^{ct814/ct814}²⁶ zebrafish lines have been previously described.

Real-Time PCR. Reverse Transcription-Polymerase Chain Reaction (RT-PCR) was performed on total RNA prepared from 20 zebrafish oocytes and embryos for each different developmental stages using the Total RNA Isolation Kit (Ambion, Thermo Fisher, Waltham MA) or the RNAgents Total RNA Isolation System (Promega, Madison, WI), treated with DNase I RNase free (Roche, Basel, Switzerland) to avoid possible contamination from genomic DNA. RNA concentrations and quality were determined using a NanoDrop ND-1000 spectrophotometer (NanoDrop Technologies Inc., Wilmington, USA). Total RNA (1 µg) was reverse transcribed to produce cDNA using Superscript III reverse transcriptase (Invitrogen) primed with random hexamers, as described previously⁴¹. In all cases, a reverse transcriptase negative control was used to test for genomic DNA contamination. The primers used for quantitative Real-Time PCR are listed in the Supplementary Table S1.

In situ hybridization. Whole-mount *in situ* hybridization (WISH) was performed as described⁴². PCR products were cloned into the pGEM-T Easy vector (Promega, Table S2). The cDNA-containing plasmids were linearized and transcribed with T7 and SP6 RNA polymerase (Roche) for antisense and sense riboprobe synthesis. Images of stained embryos were taken with a Leica MZFLIII epifluorescence stereomicroscope equipped with a DFC 480-R2 digital camera.

Knockdown experiments. We tested one antisense morpholino oligonucleotide (MO) each for *prokr1a* and *prokr1b* (Supplementary Table S3). Both were splice-blocking MOs synthesised by Gene Tools LLC (Oregon, USA). Morpholinos were dissolved in Danieau's solution (58 mM NaCl; 0,7 mM KCl; 0,4 mM MgSO₄ · H₂O; 0,6 mM Ca(NO₃)₂; 5 mM Hepes pH 7.2) at 2 mM and stored at −80 °C. Embryos were microinjected at the 1–4 cell stage with rhodamine dextran (Molecular Probes) co-injected as a tracer. As a control for non-specific effects, a standard control morpholino (*ctrl*-MO) was injected, which targets the human β -globin gene. Morpholinos were tested for efficacy and toxicity by injecting different doses in *tg(gnrh3:EGFP)* embryos and evaluating them for morphological defects (Supplementary Fig. S1A–C). After injection, embryos were raised in fish water at 28 °C and observed until the developmental stage of interest. Embryos that were to be imaged after 24 hpf were treated with PTU. For imaging, embryos were anaesthetized using tricaine (ethyl 3-aminobenzoate methanesulfonate salt, Sigma; 25x stock = 0.08 g in 20 ml of distilled H₂O) in fish water. Injected embryos (morphants) were embedded at 48 hpf in UltraPure Low Melting Point Agarose (Thermo Fisher Scientific) and photographed using a confocal laser scanning microscope (Nikon C2) with a 20x objective.

Generation of *tg(gnrh3:EGFP); prokr1b^{ct814/ct814}* line and rescue experiments. We crossed *tg(gnrh3:EGFP)*²⁷ animals to *prokr1b^{ct814/ct814}* animals²⁶ to generate the *tg(gnrh3:EGFP); prokr1b^{ct814/ct814}* line. Fin clipping was performed to isolate genetic material from individual fish for genotyping accordingly to what previous published in Chen and colleague²⁶ (Table S4). The *prokr1b^{ct814/ct814}* fish contain a 1 bp deletion (nucleotide 12 of the open reading frame: 5'-C-3'), which results in a change in reading frame after amino acid 4 and a premature stop codon after amino acid 13 compared to 396 amino acids for the wild-type (WT) protein. Rescue experiments were performed by injecting 400 pg *prokr1b* mRNA diluted in the Danieau's solution into 1-cell stage embryos.

Live-imaging of GnRH3 fibers in *prokr1b* KO embryos. To assess the role of *prokr1b* during GnRH3 fiber development, *prokr1b* KO animals were embedded at 48 or 72 hpf in UltraPure Low Melting Point Agarose (Thermo Fisher Scientific) and analysed using a confocal laser scanning microscope (Nikon C2+) with a 20x objective. GnRH3 fiber structure was assessed and 3D reconstructed using Fiji⁴³. Due to the complexity of GnRH3 fibers, a specific region of interest (ROI) was selected and analyzed at each developmental stage (Supplementary Fig. S2), with background fluorescence subtracted from each image (Supplementary Fig. S2B–D). The number of green pixels within each ROI was used as a proxy for the amount of GnRH3 fibers.

Gonads histology, fecundity/fertilization rates and GSI. For histological analysis, gonads from 3-months-old fish were fixed in 4% paraformaldehyde (PFA), dehydrated, wax-embedded, cut into 8 µm sections using a microtome (Leitz 1516), and stained with eosin. Samples were imaged using a Leica DM6000 B microscope equipped with a Leica 480 digital camera using the Leica Application Suite (LAS version 4.7.0). The assessment of fecundity (number of eggs released) and fertilization rate (fraction of eggs that developed into an embryo), WT and mutant females and males at 3 months-old were paired in a spawning tray. After one hour, eggs were collected in 30% Danieau's solution and counted. The number of fertilized and unfertilized eggs was discerned using a dissecting microscope at 6 hpf. Twelve-months-old male and female fish were then dissected to collect ovaries and testicles for gonadosomatic index (GSI) measurement and Real-time PCR. The GSI was calculated according to the formula (organosomatic index = organ weight × 100/body weight)⁴⁴.

Statistical analysis. Statistical analyses in Fig. 5 was performed using one-way ANOVA with Dunnett's post-hoc test using GraphPad PRISM version 6.0 (GraphPad, San Diego, CA). In the graphs, **P* < 0.05, ***P* < 0.01, ****P* < 0.001.

Received: 19 October 2019; Accepted: 7 April 2020;

Published: 06 May 2020

References

1. Calvin, J. L., Slater, C. H., Bolduc, T. G., Laudano, A. P. & Sower, S. A. Multiple molecular forms of gonadotropin-releasing hormone in the brain of an elasmobranch: evidence for IR-lamprey GnRH. *Peptides* **14**, 725–729 (1993).
2. Uchida, K. *et al.* Evolutionary origin of a functional gonadotropin in the pituitary of the most primitive vertebrate, hagfish. *Proc Natl Acad Sci USA* **107**, 15832–15837 (2010).

3. Takahashi, A., Kanda, S., Abe, T. & Oka, Y. Evolution of the hypothalamic-pituitary-gonadal axis regulation in vertebrates revealed by knockout medaka. *Endocrinology* **157**, 3994–4002 (2016).
4. Lethimonier, C., Madigou, T., Munoz-Cueto, J. A., Lareyre, J. J. & Kah, O. Evolutionary aspects of GnRHs, GnRH neuronal systems and GnRH receptors in teleost fish. *Gen Comp Endocrinol* **135**, 1–16 (2004).
5. Kavanaugh, S. I., Nozaki, M. & Sower, S. A. Origins of gonadotropin-releasing hormone (GnRH) in vertebrates: identification of a novel GnRH in a basal vertebrate, the sea lamprey. *Endocrinology* **149**, 3860–3869 (2008).
6. Forni, P. E. & Wray, S. GnRH, anosmia and hypogonadotropic hypogonadism—where are we? *Front Neuroendocr.* **36**, 165–177 (2015).
7. Vezzoli, V. *et al.* The complex genetic basis of congenital hypogonadotropic hypogonadism. *Minerva Endocrinol* **41**, 223–239 (2016).
8. Seminara, S. B., Hayes, F. J. & Crowley, W. F. Gonadotropin-Releasing Hormone Deficiency in the Human (Idiopathic Hypogonadotropic Hypogonadism Genetic Considerations. *Endocr. Rev.* **19**, 521–539 (1998).
9. Boehm, U. *et al.* Expert consensus document: European Consensus Statement on congenital hypogonadotropic hypogonadism—pathogenesis, diagnosis and treatment. *Nat Rev Endocrinol* **11**, 547–564 (2015).
10. Bonomi, M. *et al.* Characteristics of a nationwide cohort of patients presenting with isolated hypogonadotropic hypogonadism (IHH). *Eur J Endocrinol* **178**, 23–32 (2018).
11. Sykiotis, G. P. *et al.* Oligogenic basis of isolated gonadotropin-releasing hormone deficiency. *Proc Natl Acad Sci USA* **107**, 15140–15144 (2010).
12. Soga, T. *et al.* Molecular cloning and characterization of prokineticin receptors. *Biochim Biophys Acta* **1579**, 173–179 (2002).
13. Negri, L. *et al.* Bv8/Prokineticins and their Receptors A New Pronociceptive System. *Int. Rev. Neurobiol.* **85**, 145–157 (2009).
14. Zhou, W., Li, J.D., Hu, W. P., Cheng, M. Y. & Zhou, Q. Y. Prokineticin 2 is involved in the thermoregulation and energy expenditure. *Regul. Pept.* <https://doi.org/10.1016/j.regpep.2012.08.003> (2012).
15. Shojaei, F. *et al.* Bv8 regulates myeloid-cell-dependent tumour angiogenesis. *Nature* <https://doi.org/10.1038/nature06348> (2007).
16. Matsumoto, S. *et al.* Abnormal development of the olfactory bulb and reproductive system in mice lacking prokineticin receptor PKR2. *Proc Natl Acad Sci USA* **103**, 4140–4145 (2006).
17. Abreu, A. P., Kaiser, U. B. & Latronico, A. C. The role of prokineticins in the pathogenesis of hypogonadotropic hypogonadism. *Neuroendocrinology* **91**, 283–290 (2010).
18. Libri, D. V. *et al.* Germline prokineticin receptor 2 (PROKR2) variants associated with central hypogonadism cause differential modulation of distinct intracellular pathways. *J Clin Endocrinol Metab* **99**, E458–63 (2014).
19. Dode, C. *et al.* Kallmann syndrome: mutations in the genes encoding prokineticin-2 and prokineticin receptor-2. *PLoS Genet* **2**, e175 (2006).
20. Cole, L. W. *et al.* Mutations in prokineticin 2 and prokineticin receptor 2 genes in human gonadotrophin-releasing hormone deficiency: molecular genetics and clinical spectrum. *J Clin Endocrinol Metab* **93**, 3551–3559 (2008).
21. Abreu, A. P. *et al.* Loss-of-function mutations in the genes encoding prokineticin-2 or prokineticin receptor-2 cause autosomal recessive Kallmann syndrome. *J Clin Endocrinol Metab* **93**, 4113–4118 (2008).
22. Dode, C. & Rondard, P. PROK2/PROKR2 Signaling and Kallmann Syndrome. *Front Endocrinol* **4**, 19 (2013).
23. Martin, C. *et al.* The role of the prokineticin 2 pathway in human reproduction: evidence from the study of human and murine gene mutations. *Endocr Rev* **32**, 225–246 (2011).
24. Pitteloud, N. *et al.* Digenic mutations account for variable phenotypes in idiopathic hypogonadotropic hypogonadism. *J Clin Invest* **117**, 457–463 (2007).
25. Lin, D. C. *et al.* Identification and molecular characterization of two closely related G protein-coupled receptors activated by prokineticins/endocrine gland vascular endothelial growth factor. *J Biol Chem* **277**, 19276–19280 (2002).
26. Chen, S. *et al.* Light-Dependent Regulation of Sleep and Wake States by Prokineticin 2 in Zebrafish. *Neuron* **95**, 153–168.e6 (2017).
27. Abraham, E. *et al.* Early development of forebrain gonadotrophin-releasing hormone (GnRH) neurones and the role of GnRH as an autocrine migration factor. *J Neuroendocr.* **20**, 394–405 (2008).
28. Palevitch, O. *et al.* Nasal embryonic LHRH factor plays a role in the developmental migration and projection of gonadotropin-releasing hormone 3 neurons in zebrafish. *Dev Dyn* **238**, 66–75 (2009).
29. Biran, J., Palevitch, O., Ben-Dor, S. & Levavi-Sivan, B. Neurokinin Bs and neurokinin B receptors in zebrafish-potential role in controlling fish reproduction. *Proc Natl Acad Sci USA* **109**, 10269–10274 (2012).
30. Yanicostas, C., Herbomel, E., Dipietromaria, A. & Soussi-Yanicostas, N. Anosmin-1a is required for fasciculation and terminal targeting of olfactory sensory neuron axons in the zebrafish olfactory system. *Mol Cell Endocrinol* **312**, 53–60 (2009).
31. Kim, H. G. *et al.* WDR11, a WD protein that interacts with transcription factor EMX1, is mutated in idiopathic hypogonadotropic hypogonadism and Kallmann syndrome. *Am J Hum Genet* **87**, 465–479 (2010).
32. Liu, Y. *et al.* Genetic evidence for multifactorial control of the reproductive axis in zebrafish. *Endocrinology* **158**, 604–611 (2017).
33. Kitahashi, T., Ogawa, S. & Parhar, I. S. Cloning and expression of kiss2 in the zebrafish and medaka. *Endocrinology* **150**, 821–831 (2009).
34. Marvel, M., Spicer, O. S., Wong, T.-T., Zmora, N. & Zohar, Y. Knockout of the GnRH genes in zebrafish: effect on reproduction and potential compensation by reproductive and feeding-related neuropeptides. *Biol. Reprod.* **0**, 1–13 (2018).
35. Tang, H. *et al.* The kiss/kissr systems are dispensable for zebrafish reproduction: evidence from gene knockout studies. *Endocrinology* **156**, 589–599 (2015).
36. Svingen, T. *et al.* Prokr2-deficient mice display vascular dysmorphology of the fetal testes: Potential implications for Kallmann syndrome aetiology. *Sex. Dev.* <https://doi.org/10.1159/000335160> (2012).
37. Zhao, Y., Lin, M. C., Mock, A., Yang, M. & Wayne, N. L. Kisspeptins modulate the biology of multiple populations of gonadotropin-releasing hormone neurons during embryogenesis and adulthood in zebrafish (*Danio rerio*). *PLoS One* **9**, e104330 (2014).
38. Palevitch, O. *et al.* Cxcl12a-Cxcr4b signaling is important for proper development of the forebrain GnRH system in zebrafish. *Gen Comp Endocrinol* **165**, 262–268 (2010).
39. Westerfield, M. *The Zebrafish Book. A Guide for the Laboratory Use of Zebrafish (Danio rerio)*, 5th Edition. *Univ. Oregon Press. Eugene* (2007).
40. Kimmel, C. B., Ballard, W. W., Kimmel, S. R., Ullmann, B. & Schilling, T. F. Stages of embryonic development of the zebrafish. *Dev Dyn* **203**, 253–310 (1995).
41. Tang, R., Dodd, A., Lai, D., McNabb, W. C. & Love, D. R. Validation of Zebrafish (*Danio rerio*) Reference Genes for Quantitative Real-time RT-PCR Normalization. *Acta Biochim. Biophys. Sin. (Shanghai)*. **39**, 384–390 (2007).
42. Thisse, C., Thisse, B., Halpern, M. E. & Postlethwait, J. H. goosecoid Expression in neurectoderm and mesendoderm is disrupted in zebrafish cyclops gastrulas. *Dev. Biol.* **164**, 420–429 (1994).
43. Schindelin, J. *et al.* Fiji: An open-source platform for biological-image analysis. *Nature Methods* <https://doi.org/10.1038/nmeth.2019> (2012).
44. Gonzales, J. M. & Law, S. H. W. Feed and feeding regime affect growth rate and gonadosomatic index of adult zebrafish (*Danio rerio*). *Zebrafish* <https://doi.org/10.1089/zeb.2013.0891> (2013).

Acknowledgements

The study was supported by funds from IRCCS Istituto Auxologico Italiano (Ricerca Corrente funds: 05C623_2016) and funds from University of Milan – Dept. of Clinical Sciences and Community Health (Piano di sostegno alla ricerca - Linea 2 Azione B).

Author contributions

I.B. designed, performed and interpreted the experiments and wrote the manuscript. F.L., F.M., V.V. and L.C. performed and assisted in the experiments. D.P. provided the *prokr1b^{ct814/ct814}* mutant line and interpreted the experiments. M.B., Y.G., and L.P. conceived the study, supervised the publication, interpreted the experiments and wrote the manuscript.

Competing interests

The authors declare no competing interests.

Additional information

Supplementary information is available for this paper at <https://doi.org/10.1038/s41598-020-64077-2>.

Correspondence and requests for materials should be addressed to M.B.

Reprints and permissions information is available at www.nature.com/reprints.

Publisher's note Springer Nature remains neutral with regard to jurisdictional claims in published maps and institutional affiliations.



Open Access This article is licensed under a Creative Commons Attribution 4.0 International License, which permits use, sharing, adaptation, distribution and reproduction in any medium or format, as long as you give appropriate credit to the original author(s) and the source, provide a link to the Creative Commons license, and indicate if changes were made. The images or other third party material in this article are included in the article's Creative Commons license, unless indicated otherwise in a credit line to the material. If material is not included in the article's Creative Commons license and your intended use is not permitted by statutory regulation or exceeds the permitted use, you will need to obtain permission directly from the copyright holder. To view a copy of this license, visit <http://creativecommons.org/licenses/by/4.0/>.

© The Author(s) 2020